

RESEARCH

Open Access



# Amyloid $\beta$ oligomer induces cerebral vasculopathy via pericyte-mediated endothelial dysfunction

Siqi Chen<sup>1†</sup>, Daji Guo<sup>2,4†</sup>, Yuanyuan Zhu<sup>2†</sup>, Songhua Xiao<sup>2†</sup>, Jiatian Xie<sup>2</sup>, Zhan Zhang<sup>2</sup>, Yu Hu<sup>2</sup>, Jialin Huang<sup>2</sup>, Xueying Ma<sup>2</sup>, Zhiyuan Ning<sup>2</sup>, Lin Cao<sup>1,3\*†</sup>, Jinping Cheng<sup>2,3,4\*†</sup> and Yamei Tang<sup>2,3,4\*†</sup>

## Abstract

**Background** Although abnormal accumulation of amyloid beta (A $\beta$ ) protein is thought to be the main cause of Alzheimer's disease (AD), emerging evidence suggests a pivotal vascular contribution to AD. Aberrant amyloid  $\beta$  induces neurovascular dysfunction, leading to changes in the morphology and function of the microvasculature. However, little is known about the underlying mechanisms between A $\beta$  deposition and vascular injuries. Recent studies have revealed that pericytes play a substantial role in the vasculopathy of AD. Additional research is imperative to attain a more comprehensive understanding.

**Methods** Two-photon microscopy and laser speckle imaging were used to examine cerebrovascular dysfunction. A $\beta$  oligomer stereotactic injection model was established to explain the relationship between A $\beta$  and vasculopathy. Immunofluorescence staining, western blot, and real-time PCR were applied to detect the morphological and molecular alternations of pericytes. Primary cultured pericytes and bEnd.3 cells were employed to explore the underlying mechanisms.

**Results** Vasculopathy including BBB damage, hypoperfusion, and low vessel density were found in the cortex of 8 to 10-month-old 5xFAD mice. A similar phenomenon accompanied by pericyte degeneration appeared in an A $\beta$ -injected model, suggesting a direct relationship between A $\beta$  and vascular dysfunction. Pericytes showed impaired features including low PDGFR $\beta$  expression and increased pro-inflammatory chemokines secretion under the administration of A $\beta$  in vitro, of which supernatant cultured with bEND.3 cells led to significant endothelial dysfunction characterized by TJ protein deficiency.

<sup>†</sup>Siqi Chen, Daji Guo, Yuanyuan Zhu and Songhua Xiao authors contributed equally to this work.

<sup>†</sup>Lin Cao, Jinping Cheng and Yamei Tang share equal co-corresponding authorship.

\*Correspondence:

Lin Cao  
caolin@mail.sysu.edu.cn  
Jinping Cheng  
chengjp3@mail.sysu.edu.cn  
Yamei Tang  
tangym@mail.sysu.edu.cn

Full list of author information is available at the end of the article



**Conclusions** Our results provide new insights into the pathogenic mechanism underlying A $\beta$ -induced vasculopathy. Targeting pericyte therapies are promising to ameliorate vascular dysfunction in AD.

**Keywords** Alzheimer's disease, A $\beta$  oligomer, Blood–brain barrier (BBB), Pericytes, Tight junction proteins

## Background

Alzheimer's disease (AD) is a fatal neurodegenerative disease characterized by senile plaques, neurofibrillary tangles, and neuronal pathology [1]. Senile plaque, as a core pathology of AD, is composed of the  $\beta$ -amyloid peptide (A $\beta$ ) and abnormal tau protein [2]. Therein, amyloid-beta protein, especially A $\beta_{42}$ , is reported to be the key protein that led to the development of AD. Recent reports have proved that A $\beta$  plays an important role in AD pathology, resulting in glial activation and proliferation, neuron apoptosis, and cerebrovascular damage [3]. Most clinical treatments targeted glial and neuronal impairment in AD, such as cholinesterase inhibitors, memantine and some anti-neuroinflammatory drugs [4–6], could only enhance cognitive symptoms for a limited time period and are unable to reverse the disease course. Moreover, some of these treatments have been proven invalid, which implies an additional pathogenic mechanism of A $\beta$  protein is still yet to be discovered [7, 8].

Increasing evidence suggests a vital role for vascular disturbance in the onset of AD. Vascular compromise including hypoperfusion and blood–brain barrier (BBB) leakage occurs early in AD [9, 10]. Exogenous amyloid  $\beta$  deteriorates vascular function via amplifying neuroinflammation, activating glial cells, and disturbing endothelial metabolism [11]. On the other hand, when the structure of BBB is destroyed, the transport and degradation of A $\beta$  decline, thus enhancing A $\beta$  abnormal accumulation and forming a negative feedback loop [12, 13]. Taken together, understanding the generation mechanism of cerebral vasculopathy may open up a brand-new sight in the development and treatment of AD [14].

When it comes to vascular impairments, many previous studies have focused on endothelial cells [15, 16]. However, pericytes and pericyte-endothelial interactions also have critical roles in maintaining normal vascular function [17]. Pericyte, as a kind of mural cell in the brain, especially locates in the small vessel (arteriole, capillary, and venule) and occupies almost 80% coverage of the abluminal side of endothelial cells [18]. As the intermediary between the blood vessels and brain parenchyma, pericytes maintain the blood–brain barrier by regulating endothelial activity such as tight junction formation and transcytosis, and guiding the astrocytic end feet polarization [19]. Pericyte controls the cerebral blood flow to coordinate neurovascular coupling as it may have the ability to contract and dilate under the

stimulation of neurons [20, 21]. Besides its role in vascular function, pericyte is also found to be influential on neuroinflammatory response and metabolism [22, 23]. Regarding its vital impact on various physical activities in the brain, pericyte is believed to be relevant to many kinds of neurodegenerative diseases [24]. Unfortunately, there is limited knowledge about whether and how pericyte and pericyte-endothelial interactions are disturbed in amyloid pathology.

In this study, we explored vascular dysfunction in a transgenic AD mouse model. BBB leakage and cerebral hypoperfusion, along with pericytes and PDGFR $\beta$  decline were observed in the brains of AD mice. Further, we established a stereotaxic injection model to exclude the interference of other factors besides A $\beta$  protein. Similar vasculopathy was found in our stereotaxic injection model. The influence of A $\beta$  seen in vivo was analyzed mechanistically in cultured pericytes and endothelial cells.

## Methods

### Animals

Adult male wild type, 5x*FAD* mice, NG2-DsRed (Tg(Cspg4DsRed.T1)1A*kik*/J) mice and PDGFR $\beta$ -Cre; Ai9 (R26<sup>LSL-tdTomato</sup>) mice were obtained from the Jackson Laboratory. All the mice were of C57BL/6 background and housed in a specific-pathogen-free environment with food and water ad libitum. All animal studies were approved by the Sun Yat-sen University Animal Program Animal Care and Use Committee.

### Preparation of A $\beta$ oligomers and stereotactic injection

The preparation of A $\beta$  oligomer was based on previous studies [25, 26]. Briefly, synthetic A $\beta$ 1-42 (GenScript) was suspended in 1,1,1,3,3,3 hexafluoro-2-propanol (HFIP, Macklin, H811027) at 1 mM and the solution was divided into microcentrifuge tubes. Then the HFIP was removed by a Speed-Vac to obtain the A $\beta$  peptide films for storage. Before use, the peptide films were resuspended in DMSO at 5 mM and diluted to 100  $\mu$ M with PBS or DMEM/F12. Afterward, the mix was incubated at 4 °C for 24 h to generate oligomeric A $\beta$ . For stereotactic injection, mice ranging from 2 to 3 months were anesthetized and secured in a stereotaxic frame. After that, Mice were injected with 1  $\mu$ l of A $\beta$  (100  $\mu$ M) in the cortex (bregma: -1.35 mm, lateral: +2.00 mm, depth: -0.60 mm) using a 1701RN NEUROS SYRINGE (Hamilton) at a rate

of 0.1  $\mu\text{l}/\text{min}$ . The region within 1 mm from the injection point was defined as the A $\beta$  injection region and the area 1–4 mm away from the injection point as para-injection region in the ipsilateral cortex area.

#### Immunofluorescence staining

After perfused with ice-cold PBS, the brain tissues of mice were harvested and fixed with 4% paraformaldehyde (PFA) at 4 °C overnight. Then 20%–30% sucrose solution was used for gradient dehydration until the brains sank to the bottom. Coronal Sects. (20  $\mu\text{m}$  thick) were prepared by a freezing microtome (Leica, CryoStar NX50). After being washed with PBS three times, these brain slices were permeabilized with 0.1% Triton X-100 (Sigma) and blocked with 5% BSA (Sigma, A1933). After that, the slices were incubated with primary antibodies including mouse-anti- $\beta$ -Amyloid (BioLegend, 803,004) and rabbit-anti-PDGFR $\beta$  (Abcam, ab32570) at 4 °C overnight. Appropriate secondary antibodies (1:1000, Jackson, USA), 4,6-diamidino-2-phenylindole (DAPI, 1:1000, CST, 4083S, USA) and Lectin with DyLight™ 649 Lycopersicon Esculentum (Tomato) (Vector, DL-1178–1) were used for further staining. Images were acquired with a fluorescence microscope (Leica DM6B, Germany).

#### TUNEL staining

Apoptotic cells were detected by terminal deoxynucleotidyl transferase dUTP nick end labeling (TUNEL) assay (Promega, G3250) according to our previous study [27]. Briefly, the brain slices and cultured cells were blocked with 5% BSA and permeated in protease K solution at a concentration of 20 mg/ml for 20 min. After incubating with the TDT reaction cocktail at 37 °C in the dark for 1 h, DAPI was stained to label the nucleus.

#### Western blotting

The hippocampus and cortex of mice were extracted and lysed by RIPA buffer (Beyotime, P0013B, China) containing 1X halt™ protease and phosphatase inhibitor single-use cocktail (Invitrogen, 78,443). Afterward, Pierce™ BCA Protein Assay Kit (Invitrogen, 23,225) was used for quantitation. Samples were separated on SDS-PAGE gel and transferred to PVDF membranes (Millipore). Then we blocked the membranes with 5% milk for one hour at room temperature and incubated with primary antibodies. The primary antibodies we used include mouse-anti- $\beta$ -Tubulin (1:5000, Proteintech, 66,240–1-Ig), rabbit-anti-PDGFR $\beta$  (1:1000, Abcam, ab32570), rabbit-anti-ZO1 (1:1000, ThermoFisher, 61–7300), rabbit-anti-Occludin (1:1000, ThermoFisher, 71–1500), rabbit-anti-Claudin-5 (1:1000, Abcam, ab131259), mouse-anti-tau5 (1:5000, Invitrogen, AHB0042), and Phospho-Tau Family Antibody Sampler Kit (CST,

96628 T). Specific secondary HRP-linked antibodies (1:2000, Cell Signaling Technology, 7074S or 7076S) were subsequently incubated for an hour at room temperature.

#### Quantitative PCR

The tissues and cells were lysed with trizol reagent (Invitrogen, 15,596,018). After extraction, PrimeScript RT MasterMix (TaKaRa, RR036A) was used to turn RNA into cDNA. QPCR was performed on a CFX96 Touch Real-Time PCR Detection System. All primers used in this study are shown in Supplementary Table 1.

#### Two-photon imaging

The procedure of two-photon imaging was described in previous studies [28]. Briefly, anesthetized mice were fixed on a custom-made plate. Then a piece of skull, which is about four millimeters in diameter above the right somatosensory cortex, was removed for better imaging. 4kD and 70kD Dextran dye (Sigma-Aldrich) was injected via suborbital venous plexus. 2 to 3 fields were imaged per mouse using an Olympus 2-photon imaging system (Olympus SW FV31S, Japan).

#### Laser speckle imaging

According to our previous study [29], after anesthesia with isoflurane, mice were placed on a heating pad to keep warm under the probe. Then we exposed the skull and removed the hair to acquire a clear vision. The situation of perfusion was measured by PeriCam PSI blood flow imaging software (Perimed AB, Jarfalla, Sweden).

#### Cell culture and treatment

Murine pericytes were isolated as previously reported [30]. Briefly, the cortex of 3–4 weeks wild type C57BL/6 J mice were extracted and digested for half an hour by Collagenase II (Solarbio, C8150) to isolate microvessels. The cells were then cultured in a medium containing Dulbecco's Modified Eagle Medium (DMEM, GIBCO, C11965500BT), 10% fetal bovine serum (GIBCO, 10099141C), 1% N2-supplement (GIBCO, 17,502,048), mouse recombinant EGF (Sino Biological, 50,482-MNAY), recombinant murine FGF-basic (PeproTech, 450–33-10).

#### Statistical analysis

Statistical chart were produced by Prism 9.0 (GraphPad Software, San Diego, CA) and presented as mean  $\pm$  SEM. Unpaired two-tailed Student's t-test was used for two-group comparison and one-way ANOVA was performed for multiple comparisons analysis using SPSS software (IBM). Vascular analysis was accessed by Angiotool software [31]. Statistical significance was taken as \*( $p < 0.05$ ), \*\* ( $p < 0.01$ ), \*\*\* ( $p < 0.001$ ) and \*\*\*\* ( $p < 0.0001$ ).

## Results

### Vasculopathy was observed in the brains of 8-10mo 5xFAD mice

As a commonly used transgenic AD mouse model, 5xFAD mice were proved to have cognitive decline and A $\beta$  plaque deposition at the age of 8–10 months [32]. To access the vascular change in 8-10mo 5xFAD mice, we first used two-photon imaging and laser speckle imaging technologies to visualize the structure and perfusion of cerebral vessels.

70kD Rhodamine-dextran was injected retro-orbitally into the 5xFAD mice and their cagemate wild type (WT) mice to display the vascular morphology and the 4kD FITC-dextran was used to evaluate the BBB permeability. When BBB broke down, intravascular 4kD FITC-dextran would leak into cerebral parenchyma while 70kD Rhodamine-dextran remained in the vascular lumen. We observed that for 5xFAD mice, the fluorescent signal of 4kD FITC-dextran dye was immediately detected in the perivascular region of the brain parenchyma and kept increasing with the extension of imaging time, suggesting a continuous BBB leakage in 5xFAD mice. Conversely,

rare FITC-dextran dye was found in WT mice (Fig. 1A). Data showed the concentration of dye in the perivascular region of AD mice was about 1.5 times that of the WT mice 30 min after injection (Fig. 1B, C). Further analysis illustrated that the total vessel length ( $p < 0.01$ ) and coverage area ( $p < 0.05$ ) (Fig. 1D, E) were decreased in the cortex of 5xFAD mice. Laser speckle imaging showed that compared with WT mice, cerebral perfusion of 8-10mo 5xFAD mice significantly decreased (Fig. 1F, G) ( $p < 0.01$ ), which was consistent with the loss of vessels density.

All these findings provided evidence that 8-10mo 5xFAD mice have remarkable vasculopathy, including BBB disruption, hypoperfusion and low vessel density.

### Vascular PDGFR $\beta$ deficiency was found in the brains of 8-10mo 5xFAD mice

Since pericytes are important for BBB integrity and capillary constriction [33, 34], we next explored the alteration of pericytes in 5xFAD mice. According to previous studies, PDGFR $\beta$ , which was mainly expressed in capillary pericytes in the brain, was used as the marker of pericytes [35]. Immunofluorescence staining results demonstrated

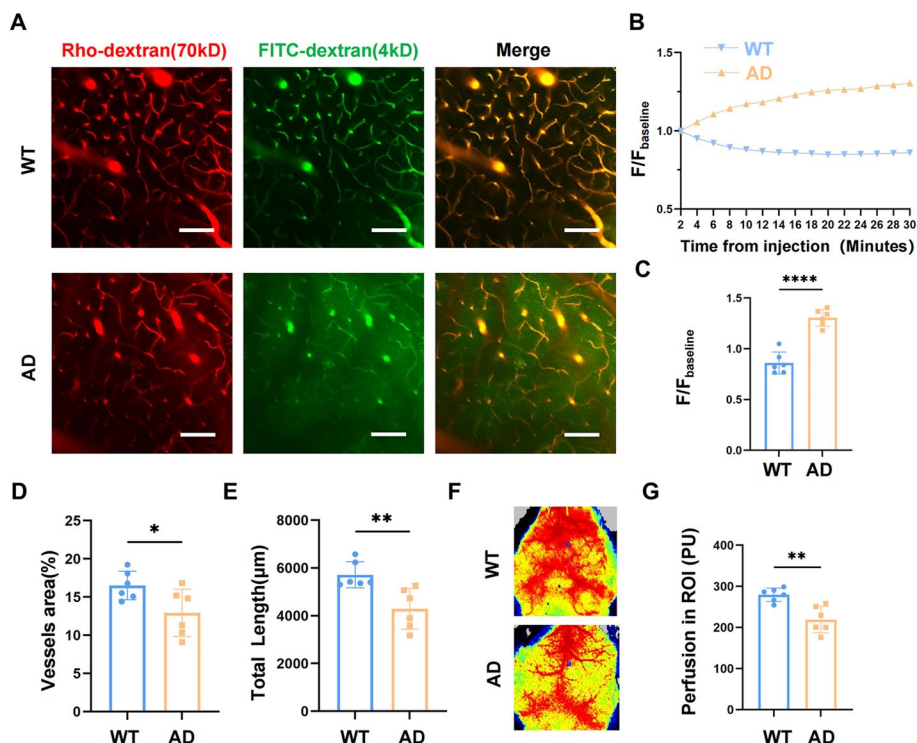


**Fig. 1** Vasculopathy was observed in the brains of 8-10mo 5xFAD mice. **A** Representative two-photon images showed cerebral vasculature and BBB breakdown in the somatosensory cortex of 8-10mo 5xFAD mice. 70kD Rhodamine-dextran was shown in red and 4kD FITC-dextran dye was in green. Scale bar: 100  $\mu$ m. **B** Variation curve of the total extravascular 4kD FITC-dextran signal intensity after retro-orbital injection. **C** Volumetric quantification of FITC-dextran extravasation 30 min after injection. **D-E** Quantitative analysis of total vessel coverage area and length in the cortex of both groups. **F** Representative laser speckle images demonstrated the situation of cerebral perfusion. **G** Quantification of cerebral perfusion in ROI. All the data were presented as mean  $\pm$  SEM and analyzed using unpaired t test.  $n = 6$  for each group. \*  $p < 0.05$ , \*\*  $p < 0.01$ , \*\*\*  $p < 0.001$  and \*\*\*\*  $p < 0.0001$

an evident A $\beta$  protein deposition alongside the loss of PDGFR $\beta$  signal in the hippocampus CA1 region and cortex of the AD mice model (Fig. 2A, B). Although the number of PDGFR $\beta$ <sup>+</sup> cells remained constant, the percentage of PDGFR $\beta$ <sup>+</sup> area covering lectin-labeled vessels

dramatically declined no matter in the hippocampus ( $p < 0.01$ ) or the cortex ( $p < 0.01$ ) of 8-10mo 5xFAD mice (Fig. 2C).

We further confirmed the mRNA and protein level of PDGFR $\beta$  by qPCR and Western blotting respectively.

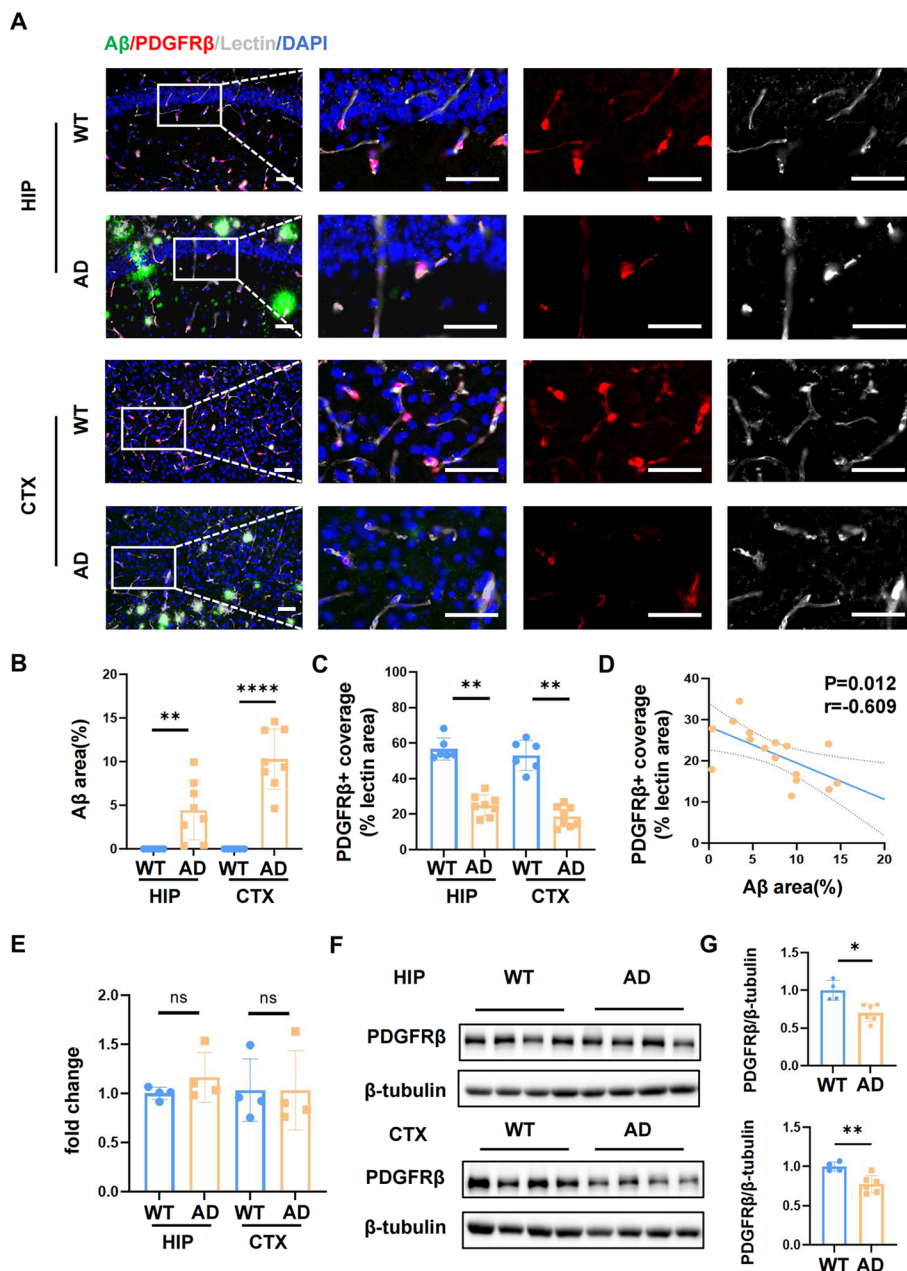


**Fig. 2** Vascular PDGFR $\beta$  deficiency was found in the brains of 8-10mo 5xFAD mice. **A** Representative immunofluorescent staining images of PDGFR $\beta$  (red), A $\beta$  (green) and lectin (grey) co-labeling in the hippocampus (upper panel) and cortex (low panel) of 8-10mo wild type ( $n=6$ ) and 5xFAD ( $n=8$ ) mice. Scale bar: 50  $\mu$ m. **B** Quantification of A $\beta$ -positive area in both groups. **C** Quantification of PDGFR $\beta$ -positive coverage area. **D** Pearson's coefficient ( $r$ ) correlation analysis between the percentage of PDGFR $\beta$ <sup>+</sup> area and A $\beta$ <sup>+</sup> area in the cortex of AD mice. **E** Quantitative analysis of PDGFR $\beta$  mRNA levels.  $n=4$  for each group. **F-G** Western blotting analysis of PDGFR $\beta$  protein expression level in the hippocampus (upper panel) and cortex (low panel) of wild type ( $n=4$ ) and 5xFAD mice ( $n=6$ ). Data are shown as mean  $\pm$  SEM. \* $p < 0.05$ , \*\* $p < 0.01$ , \*\*\* $p < 0.001$ , and \*\*\*\* $p < 0.0001$

Data revealed that the mRNA level of PDGFR $\beta$  stayed the same (Fig. 2E), while the protein level of PDGFR $\beta$  decreased in the CA1 region ( $p < 0.05$ ) and cortex ( $p < 0.01$ ) of 5xFAD mice compared to WT controls (Fig. 2F, G). Surprisingly, the PDGFR $\beta$  protein level was cut down more obviously in the cortex region. Interestingly, Pearson's correlation analysis implied that PDGFR $\beta$  loss was possibly associated with A $\beta$  deposition area in the cortex of 5xFAD mice ( $p < 0.05$ ). This suggested that vascular PDGFR $\beta$  deficiency in AD might be attributed to the vasotoxic effects of A $\beta$  protein.

#### **A $\beta$ oligomer injection induced BBB leakage and local cortex hypoperfusion in 2mo WT mice**

To further characterize the role of A $\beta$  protein in cerebrovascular dysfunction and eliminate the effects of other pathogenic factors in AD, we established a stereotactic injection model (Fig. 3A, Supplementary Fig. 1A). First, soluble A $\beta$ 42 protein was processed into oligomer for A $\beta$  oligomer (A $\beta$ o) was proved to be more toxic than A $\beta$  monomer and fiber in both neuronal [36–38] and vascular level [39, 40]. Dot blotting was used to confirm that A $\beta$ o was produced successfully (Supplementary Fig. 1B). Then we injected A $\beta$ o into the cortex of two-month-old mice to mimic A $\beta$  pathology in AD and further confirmed the success of injection by immunofluorescence staining immediately after the operation (Supplementary Fig. 1C). To rule out the influence of stereotactic injection, we injected the solvent of A $\beta$ o (2%DMSO) as a better control group.

Two-photon imaging revealed that the solvent administration group did not exist BBB leakage after recovering from injection for a month. There was almost no difference between the DMSO group and the control group without any treatment. On the contrary, the A $\beta$ o administration group showed remarkably increased BBB permeability ( $p < 0.01$ ) (Fig. 3B–D). Interestingly, we found that the total vessel area and length did not change (Fig. 3E, F), suggesting that the decreased capillary density might be a delayed symptom in AD and might appear after a longer A $\beta$ o treatment time. We, therefore, focused on the perfusion situation in this stereotactic injection model. It is worth noting that compared to the contralateral side, A $\beta$ o injection induced local cortex hypoperfusion around the injection point (Fig. 3G, H) ( $p < 0.01$ ). Previous studies have demonstrated that A $\beta$  has great influence in tau oligomerization, aggregation and phosphorylation [41]. Additionally, there is increasing evidence that the abnormal tau proteins also take part in BBB breakdown [42]. Thus, we detected the protein levels of total tau and phosphorylated tau at residues Ser202/Thr205, Thr181, Ser396 in the cortex of A $\beta$ o-injected wild type mice, as well as in healthy controls. The results

showed no significant changes in the levels of all these proteins one month after A $\beta$  oligomer injection (Supplementary Fig. 1D, E). These findings indicated that in our study, a single stereotactic injection of A $\beta$  was insufficient to induce an increase in tau pathology, suggesting that A $\beta$  itself may contribute to the vasculopathy seen in AD. All these results claimed that we successfully established a model to imitate vascular dysfunction in AD and proved that A $\beta$  was able to result in vasculopathy independently.

#### **NG2 expression decreased after A $\beta$ o injection in NG2-DsRed mice**

We next used NG2-DsRed mice to examine whether there existed pericyte loss in this A $\beta$ o stereotactic injection model. Similar to PDGFR $\beta$ , NG2 is another pericyte marker [43]. We observed that the NG2-positive signal dramatically diminished in the A $\beta$ o injection region compared with the DMSO group (Fig. 4A). NG2-positive cells reduced by about 20% in the A $\beta$ o-injected region (Supplementary Fig. 2B). Furthermore, the percentage of coverage length and area of NG2-positive cells notably declined at the injection point (Fig. 4B, C) ( $p < 0.001$ ,  $p < 0.0001$ ). It was interesting that the length and area of NG2-positive cells also downregulated after A $\beta$ o administration in the para-injection region, which was defined as the ipsilateral cortex area 1–4 mm away from the injection point (Fig. 4D, E) ( $p < 0.001$ ,  $p < 0.001$ ). The number of NG2-positive cells in the para-injection region also decreased in the A $\beta$ o group (Supplementary Fig. 2B). We speculated that this phenomenon was attributed to the propagation of A $\beta$  as indicated by previous studies [44, 45]. Tunel staining suggested that the change of NG2 was not owing to pericyte apoptosis (Supplementary Fig. 2A). These results above indicated that A $\beta$ o injection inhibited the expression of NG2 around the injection point.

#### **A $\beta$ o injection inhibited the expression of PDGFR $\beta$ and induced an inflammatory response in PDGFR $\beta$ -cre: Ai9 mice**

In consideration of their high heterogeneity, pericytes are still hard to identify in the brain today [18]. To ensure the loss of the NG2 signal was due to the pericyte degeneration, we used another transgenic mouse model, which was obtained from the PDGFR $\beta$ -cre mice crossed with Ai9 reporter mice, to label pericytes. Immunofluorescence staining detected a similar decrease in PDGFR $\beta$ -positive cells coverage in lectin<sup>+</sup> length ( $p < 0.0001$ ) and area ( $p < 0.001$ ) in the A $\beta$ o injection region (Fig. 5A, C, D). What's more, the number of PDGFR $\beta$ -positive cells declined significantly compared with the DMSO group. Interestingly, the total length of the lectin<sup>+</sup> area shows no significant change between A $\beta$ o injection and control groups (Fig. 5B), which is correlated with the former

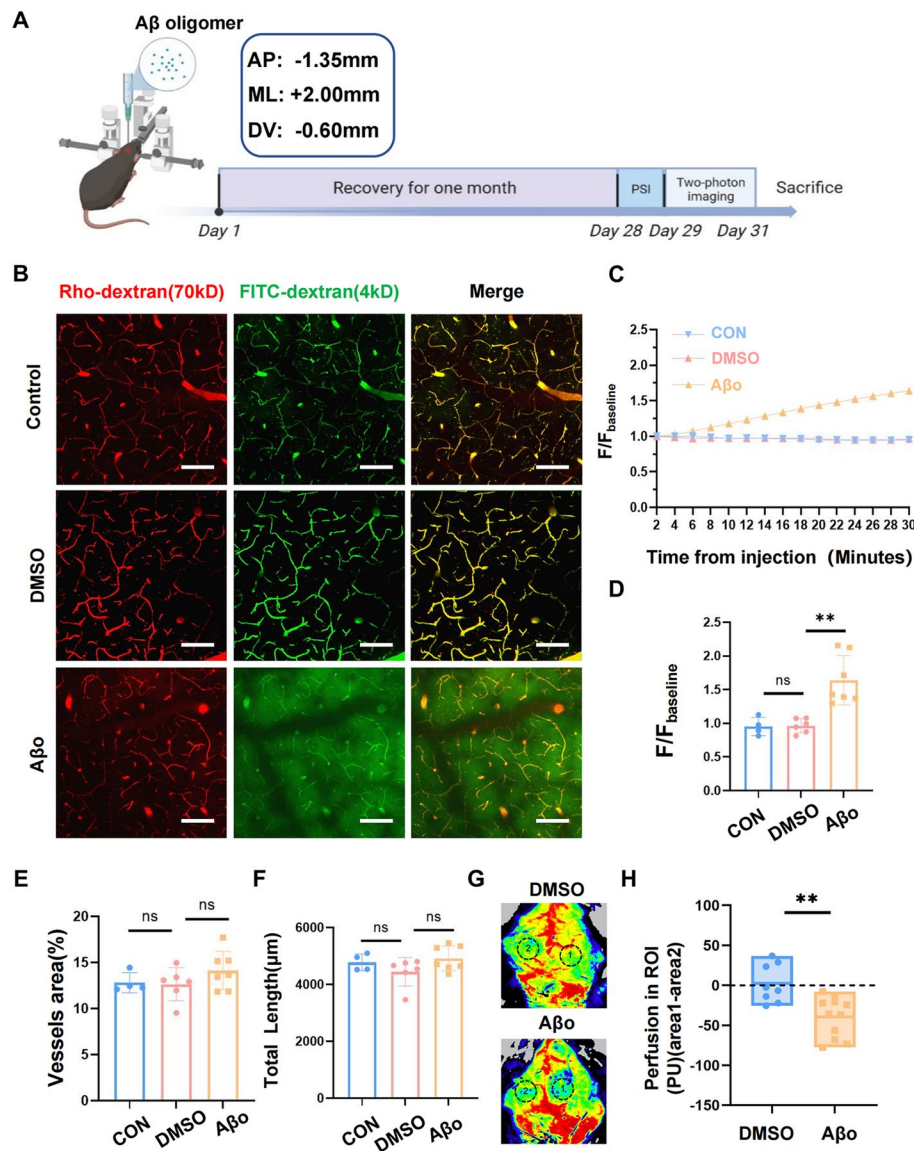


**Fig. 3** A $\beta$  oligomer stereotactic injection induced BBB leakage and local cortex hypoperfusion in 2mo WT mice. **A** Schematic diagram of the experiment design. **B** Representative in vivo two-photon images of the cortex of mice in control ( $n=4$ ), vehicle (2%DMSO) ( $n=6$ ), and A $\beta$ o-injected ( $n=7$ ) groups. 2–3 stacks were acquired to obtain the mean for each animal. Scale bar: 100  $\mu$ m. **C** Variation curve of extravasated FITC-dextran dye intensity in these three groups after injection. **D** Quantitative analysis of FITC-dextran extravasation 30 min after injection. **E–F** Quantification of cortical vascular length and area from the three experimental groups. **G** Representative laser speckle images of DMSO ( $n=8$ ) and A $\beta$ o ( $n=11$ ) groups. **H** Quantification of D-value of cerebral perfusion between injection region (ROI 1) and contralateral cortex (ROI 2) in DMSO and A $\beta$ o groups. D-value was defined as the ROI 1 quantitative perfusion value minus ROI 2. All the data were presented as mean  $\pm$  SEM. \* $p < 0.05$ , \*\* $p < 0.01$ , and \*\*\* $p < 0.001$

result we observed from the two-photon microscope, indicating that administration of A $\beta$ o influenced pericytes more severely and rapidly than endothelial cells. Furthermore, we extracted the hypoperfusion brain tissue about 4 mm in diameter according to laser speckle imaging results. Western blotting revealed significant down-regulation of PDGFR $\beta$  expression ( $p < 0.05$ ) after A $\beta$ o injection (Fig. 5E, F). Consistent with our data

in AD mice, the mRNA level of PDGFR $\beta$  did not show any difference (Fig. 5G), indicating that the alternation of PDGFR $\beta$  was only limited to the protein level. Taken together, we found that pericytes underwent degeneration in our A $\beta$ o injection model.

Neuroinflammation was considered to play a key role in the progression of AD [46]. To examine the effects

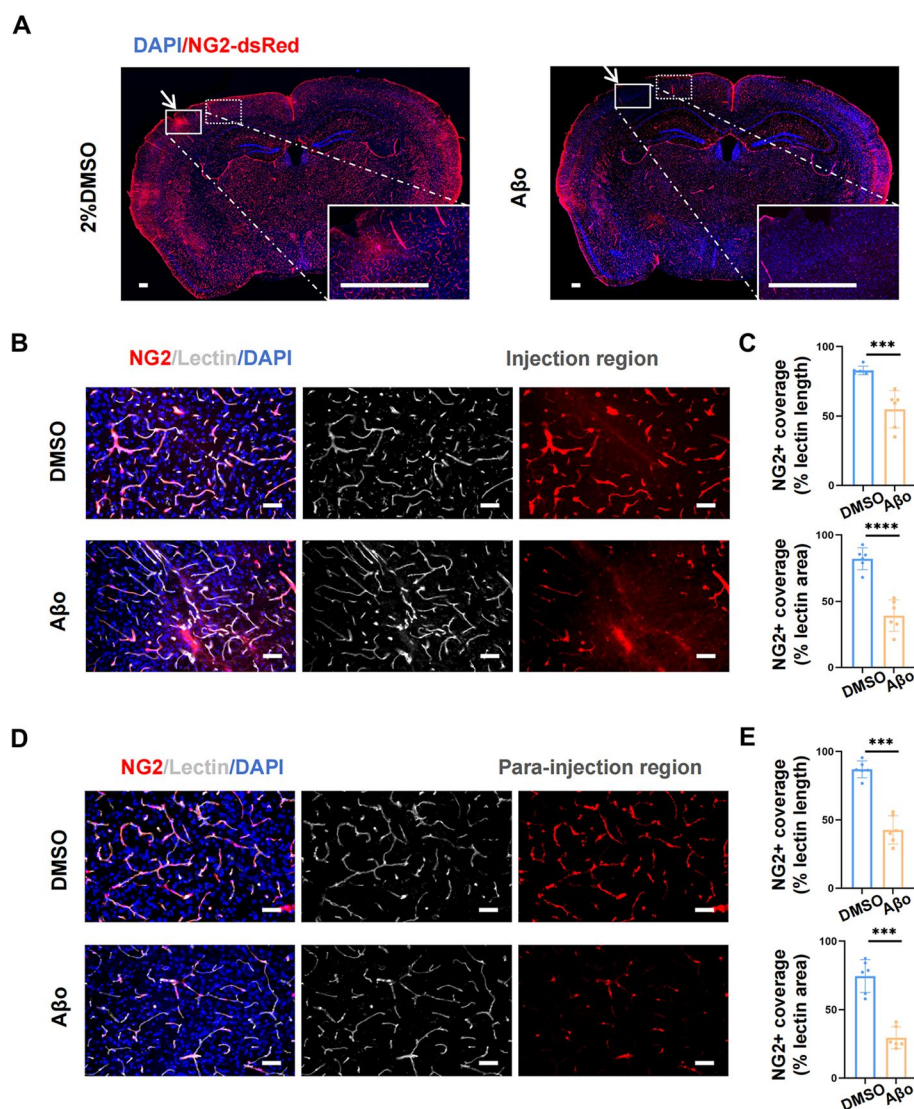


**Fig. 4** The level of NG2 expression decreased after A $\beta$  injection in NG2-DsRed mice. **A** Representative images of coronal brain section of the vehicle (2%DMSO) and A $\beta$ -injected NG2-DsRed mice. The area 1 mm around the injection point (the arrow points) was defined as the injection region and the ipsilateral cortex area 1-4 mm away from the injection point was defined as the para-injection region. Scale bar: 250  $\mu$ m **B** Representative immunofluorescent staining images of NG2 (red) and lectin (grey) in the injection region of both groups. Scale bar: 50  $\mu$ m **C** Quantification of NG2-positive coverage length (upper panel) and area (low panel) in the injection region of both groups. **D** Representative immunofluorescent staining images of NG2 (red) and lectin (grey) in the para-injection region of both groups. Scale bar: 50  $\mu$ m **E** Quantification of NG2-positive coverage length (upper panel) and area (low panel) in the para-injection region of both groups. All the data were presented as mean  $\pm$  SEM and analyzed using an unpaired t-test.  $n=6$  for each group. \* $p < 0.05$ , \*\* $p < 0.01$ , \*\*\* $p < 0.001$  and \*\*\*\* $p < 0.0001$

of A $\beta$  in neuroinflammation, we detected the mRNA level of some classic inflammatory cytokines in our stereotaxic injection model. There is no difference in IL6 or IL10 between the DMSO and the A $\beta$  group, while the mRNA levels of TNF $\alpha$  ( $p < 0.05$ ), CCL2 ( $p < 0.05$ ), CXCL10 ( $p < 0.05$ ) were significantly elevated (Fig. 5H). These findings revealed that A $\beta$  exaggerated neuroinflammation in the injection area.

#### Pericytes incubated with A $\beta$ demonstrated a proinflammatory profile and affected endothelial cells via reducing tight-junction proteins in vitro

To further confirm that A $\beta$  was able to reduce the expression of PDGFR $\beta$  in pericytes, primary cultured pericytes were incubated with A $\beta$  for 24 h and 72 h at a concentration of 10  $\mu$ M in vitro. Consistent with the results above, the level of PDGFR $\beta$  slightly declined after 24 h and remarkably reduced three days after

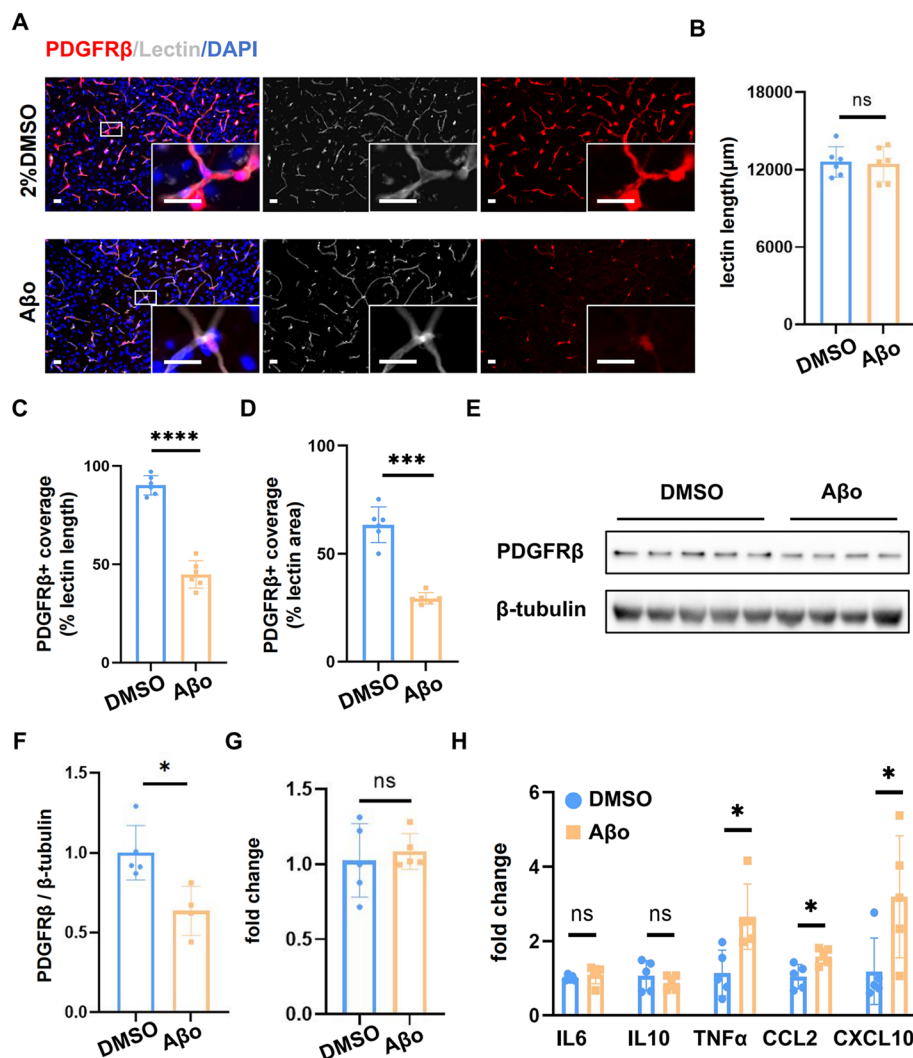


**Fig. 5** Aβo injection inhibited PDGFRβ expression and induced an inflammatory response in PDGFRβ-cre: Ai9 mice. **A** Representative immunofluorescent staining images of PDGFRβ (red) and lectin (grey) in the injection region of vehicle (2%DMSO) and Aβo-injected NG2-DsRed mice. Scale bar: 20 μm **B** Quantification of the total length of lectin<sup>+</sup> area. **C-D** Quantification of PDGFRβ<sup>+</sup> coverage length (left panel) and area (right panel) in the injection region of both groups. **E-F** Western blotting analysis of PDGFRβ protein expression level in brain tissues after 2%DMSO and Aβo injection. **G** QPCR analysis of PDGFRβ mRNA expression level in brain tissues after vehicle and Aβo injection. **H** QPCR analysis of mRNA levels of some classic inflammatory factors (IL6, IL10, TNFα, CCL2, CXCL10) in brain tissues. All the data were presented as mean ± SEM and analyzed using an unpaired t-test. *n* = 6 for each group. \* *p* < 0.05, \*\* *p* < 0.01, \*\*\* *p* < 0.001 and \*\*\*\* *p* < 0.0001

Aβo treatment (Fig. 6A, B) (*p* < 0.01). We first explored whether the decline of PDGFRβ was due to the death of pericytes. The viability of pericytes detected by the CCK-8 assay decreased proportionally with treatment time and concentration while incubating with Aβ oligomers (Supplementary Fig. 3A). TUNEL staining illustrated that rare pericytes underwent apoptosis after Aβo treatment (Supplementary Fig. 3B). Next, we used qPCR to investigate possible mediators between pericytes and endothelial cells according to the comparative cDNA expression array data in a previous study [47]. We found

that the mRNA levels of some traditional inflammatory cytokines, such as IL6, IL10, IL1β, TNFα, and TGFβ, demonstrated an increasing trend in pericytes incubated with Aβo for three days. Besides, some cytokines associated with cell death, including cyclin D1 (CCND1) and defender against cell death-1 (DAD-1), were also elevated. Among those potential genes, the changes in chemokine family expression in pericytes were noticeably higher than the other genes. The mRNA level of CCL2 in pericytes treated with Aβo for 72 h was about four times more than that of the control group. For

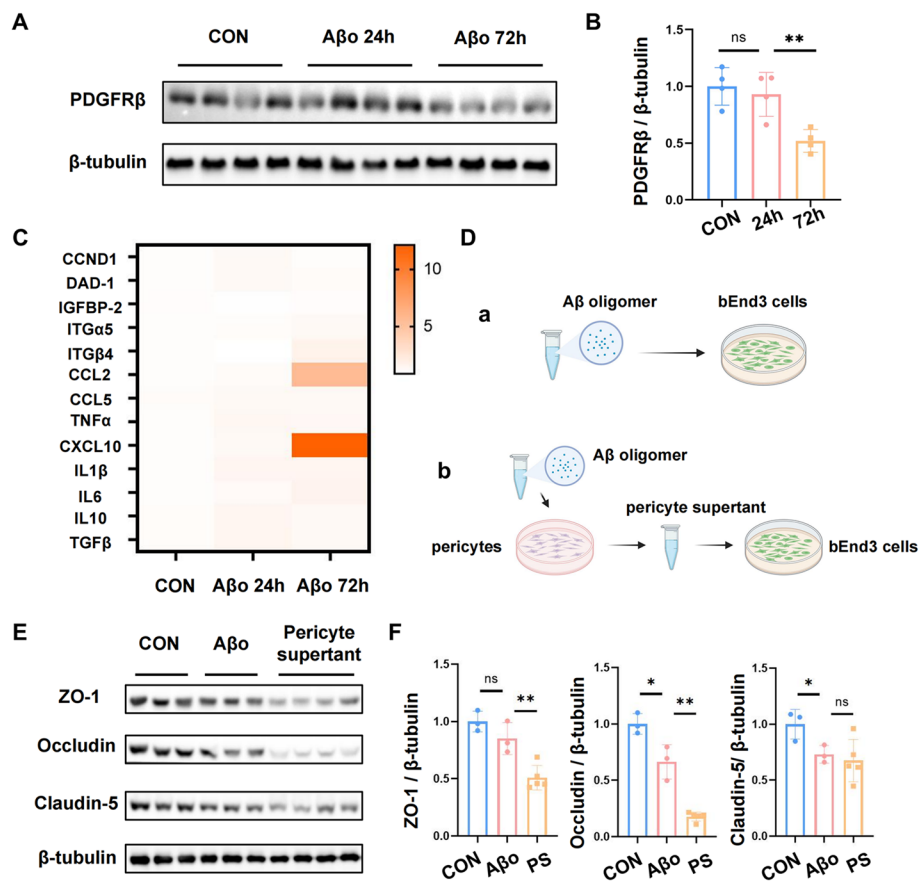


**Fig. 6** Aβo-incubated pericytes demonstrated a proinflammatory profile and decreased tight-junction proteins in endothelial cells in vitro. **A–B** Western blotting analysis of PDGFRβ protein expression level in primary cultured pericytes incubated with Aβo for 24 h and 72 h. **C** Heat map summary of Aβo-stimulated genes in primary pericytes incubated with Aβo for 24 h and 72 h. **D** Schematic diagram of bEnd3 cells incubated with primary pericytes supernatant. **E–F** Western blotting analysis of tight junction protein (ZO-1, Claudin-5, and Occludin) expression levels in bEnd3 cells incubated with Aβo and primary pericytes supernatant. All the data were presented as mean ± SEM. \*  $p < 0.05$ , \*\*  $p < 0.01$

CXCL10, the gene expression reached approximately 10 times (Fig. 6C). These findings showed that Aβo inhibited the expression of PDGFRβ and raised the secretion of inflammatory factors in primary pericytes.

Moreover, we sought to evaluate whether the TJ proteins in bEnd.3 cells underwent degeneration after incubating with the supernatant of pericytes treated with Aβo. Given that Aβo has been implicated with the decrease of TJ proteins in endothelial cells [48], we added a group of bEnd.3 cells which were incubated with Aβo at a dose of 10 μM for better comparability (Fig. 6D). Unsurprisingly, the expression of TJ proteins, including ZO-1, Occludin ( $p < 0.05$ ) and Claudin 5 ( $p < 0.05$ ), was reduced after Aβo administration. Importantly, after incubating with the supernatant of Aβo-treated pericytes, bEnd.3 cells demonstrated much lower protein levels of ZO-1 ( $p < 0.01$ ), Occludin ( $p < 0.01$ ) and Claudin 5 (Fig. 6E, F). Together, these data suggested that pericytes incubated with Aβo aggravated the injury of TJ proteins in endothelial cells.

## Discussion

Ever since George G. Glenner and Caine W. Wong discovered the Aβ protein in the brains of AD patients in 1984 [49], the downstream mechanisms of this abnormal-folded protein attracted a lot of attention internationally. To cure this fatal neurodegenerative disease, therapies targeting the Aβ protein have been hot spots for a long time. However, many drugs failed to reach the expectation of slowing down the progress of AD in clinical trials, raising doubts about the “amyloid cascade hypothesis” [50, 51]. Some researchers believe that Aβ acts more like a trigger or accelerator rather than a direct cognitive effector in AD [52]. On the contrary, they consider that the miss-folded tau protein, as another important pathological protein, has a more important influence on cognitive function due to its neuronal and synapse toxicity [53]. Recently, a successful phase 3 clinical trial of donanemab, an Aβ monoclonal antibody, restored faith in the Aβ hypothesis. Among participants at the

early stage of AD, donanemab was proven to slow clinical progression at 76 weeks [54]. In addition, ACI-24, an anti-A $\beta$  vaccine, received fast-track approval from the U.S. Food and Drug Administration (FDA) on June 27, 2023 [55]. All these successful trials reconfirm the vital role of A $\beta$  in AD and indicate a bright future for anti-A $\beta$  therapies. In our study, we strengthened the reliability of anti-A $\beta$  therapies by providing new insight into its vasotoxicity in A $\beta$ -related pathology. We revealed a relationship between A $\beta$  pathology and cerebral vasculopathy in 5xFAD mice and an A $\beta$ -injected mouse model, identified the associated molecular changes in pericytes and explored the underlying mechanisms.

Vascular dysfunction, including BBB leakage and reduction in cerebral blood flow, is reported to play an important role in the progress of AD [56, 57]. Vasculopathy is not exclusive to the later clinical symptoms of AD, but also happens in patients with early amyloid and tau pathology [14]. A retrospective study has found patients with cerebrovascular accidents suffer a much higher risk of AD than others [58]. According to a previous clinical study, BBB injury was considered as one of the early biomarkers of cognitive impairment in AD patients [59]. BBB leakage allows infiltration of peripheral immune cells into the brain, and accumulation of peripheral protein and poisonous substance in cerebral parenchyma, such as fibrinogen, globulin, and exogenous A $\beta$  protein, both of which contribute to neuroinflammation and neuronal damage [60, 61]. Non-structural vascular abnormalities also took a considerable part in AD. Hemodynamic abnormalities such as hypoperfusion and microthrombosis induce regional hypoxia and neurovascular uncoupling, hence worsening the process of AD [14, 62]. In our research, we first detected BBB breakdown and hypoperfusion in 8-10mo 5xFAD mice, supporting the concept that vasculopathy indeed appeared in the process of AD. To find out the cause of BBB leakage, we used immunofluorescence staining and western blot to identify PDGFR $\beta$  deficiency in the brain capillaries of 5xFAD mice. PDGFR $\beta$  deficiency implied that there might be a pericyte loss or detachment in microvessels. This is consistent with a previous study that uncovered that pericyte implantation increased cerebral perfusion and alleviated A $\beta$  pathology in AD model mice [63]. Angio-analysis recovered that in AD mice, the total length and area of brain vessels were decreased, which partly explained the hypoperfusion phenomenon, but whether decreased vessel density, hypoperfusion and later hypoxia are sufficient to be responsible for AD-related neuronal impairment needs further examination. Of note, the possible locational co-relation of A $\beta$  deposits and PDGFR $\beta$  loss in 5xFAD mice gave us a hint that the relationship between pericytes and A $\beta$  was worth to be explored.

As a composition of BBB, pericytes were of great importance in vascular homeostasis [33]. BBB-associated pericytes were able to clear A $\beta$  deposition via an LRP1-dependent ApoE isoform-specific pathway [64]. Unfortunately, only a few studies focused on the relationship between A $\beta$  and pericytes [65]. Previous research disclosed that A $\beta$  oligomers evoked ROS generation in pericytes, thus increasing the release of endothelin-1 (ET-1). The increasing level of ET-1 was associated with pericyte contraction, resulting in constriction at the pericyte location in human capillaries [25, 66]. Moreover, several studies suggested that A $\beta$  protein enhanced the level of matrix metalloproteinase-9 (MMP-9), increased the activity of caspase 3/7, decreased viability and proliferation, and even led to death in pericytes [39, 67]. Herein, we set up a model to uncover the direct relationship between A $\beta$  protein and vascular pathology via injecting A $\beta$ o into the brain cortex. Interestingly, we found significant differences in the expression of PDGFR $\beta$  and NG2 accompanied with similar hypoperfusion and BBB breakdown in this mouse model, suggesting that pericytes indeed took an important part in A $\beta$ -induced vasculopathy.

When it comes to the mechanisms underlying pericyte-associated BBB breakdown, we first examined whether there existed pericyte death after A $\beta$  treatment. To our surprise, Tunel staining showed rare cell apoptosis appeared in our model. Besides, the number of pericytes decreased slightly while the coverage of pericytes significantly changed. All these dropped a hint that non-structural changes in pericytes might be the leading part of the pathogenesis. Similar to endothelial cells, pericytes also function as an important regulator of microenvironment homeostasis through secreting several factors. Pericytes were proved to be the first responder to systemic inflammation. Immediately after LPS injection, pericytes rapidly secreted chemokine CCL2 and were the major source of inflammatory factors within the first two hours [68]. Another research in the brains of cocaine abusers illustrated that pericytes, other than endothelial cells, played a vital role in expressing CXCL10, which brought about monocyte infiltration and NF- $\kappa$ B-related neuroinflammation [69]. According to a previous in-vitro study, human brain pericytes showed separate gene expression after incubating with A $\beta$ o [47]. We observed similar alternations in mouse primary pericytes in vitro. The expression of CCL2, CXCL10, and other inflammatory factors was significantly raised after A $\beta$ o administration. These changes increased over time and further studies are needed to verify their influence.

### Limitations of the study

While our study is a meaningful step in A $\beta$ -induced pathology, it also has some limitations. One concern about the findings was that the number of mice used to evaluate the situation of cerebral vasculopathy and pericyte loss was kept low for feasibility and ethical purposes. What's more, we did not put our emphasis on the hippocampus-associated changes and cognitive dysfunction because we focused on the alternation of the somatosensory cortex due to the limited detection depth of two-photon imaging technology. Lastly, more experiments were needed to explore the underlying mechanisms of the interactions between pericytes and endothelial cells.

### Conclusions

Taken together, our work identified evident vasculopathy and PDGFR $\beta$  deficiency in 8-10mo 5xFAD mice. Along with pericyte degeneration, an A $\beta$  stereotactic injection mouse model demonstrated similar vascular dysfunction such as BBB leakage and hypoperfusion. The increased levels of inflammatory factors in pericytes after A $\beta$  treatment inhibited the expression of TJ proteins in endothelial cells. We revealed that targeting pericyte therapies may be promising strategies for the prevention and therapy of A $\beta$ -induced vasculopathy.

### Abbreviations

AD	Alzheimer's disease
A $\beta$	Amyloid- $\beta$
BBB	Blood-brain barrier
PDGFR $\beta$	Platelet-derived growth factor receptor- $\beta$
TJ	Tight-junction
WT	Wild type
A $\beta$ o	Amyloid beta oligomer
CCND1	Cyclin D1
DAD-1	Defender against cell death-1
MMP-9	Metalloproteinase-9
ET-1	Endothelin-1

### Supplementary Information

The online version contains supplementary material available at <https://doi.org/10.1186/s13195-024-01423-w>.

**Additional file 1: Figure S1.** Dot blotting and immunofluorescent staining to ensure successful A $\beta$  oligomerization and effective injection. A. Schematic diagram of the A $\beta$ o injection point B. Representative images of dot blotting. C. Representative immunofluorescent staining images of A $\beta$  (green) and DAPI at the injection point 10 min and 30 min after A $\beta$ o treatment. Scale bar: 50  $\mu$ m D-E. Western blotting analysis of total tau (tau5) and phosphorylated tau at residues Ser202/Thr205 (AT8), Thr181, Ser396 expression levels in the injection cortex. All the data were presented as mean  $\pm$  SEM.

**Additional file 2: Figure S2.** The number of pericytes declined after A $\beta$ o treatment and rare apoptosis was found in A $\beta$ o-injected NG2-DsRed mice. A. Representative images of NG2 (red), tunel (green) and DAPI (blue) in the injection region and para-injection region of vehicle (2%DMSO) and A $\beta$ o-injected NG2-DsRed mice. B. Quantification the number of NG2 + cells/(mm<sup>2</sup>) in the injection region and para-injection region of the

vehicle (2%DMSO) ( $n=6$ ) and A $\beta$ o-injected ( $n=6$ ) groups. C. Quantification of the number of PDGFR $\beta$  + cells/(mm<sup>2</sup>) in the injection region of vehicle (2%DMSO) ( $n=6$ ) and A $\beta$ o-injected ( $n=6$ ) groups. All the data were presented as mean  $\pm$  SEM and analyzed using an unpaired t-test. \*\*  $p < 0.01$  and \*\*\*\*  $p < 0.0001$

**Additional file 3: Figure S3.** The viability of primary pericytes decreased after A $\beta$ o incubation and rare apoptosis was found in vitro. A. The OD value (450 nm) of primary pericytes detected by CCK-8 assay after incubated in media containing different concentrations of A $\beta$  oligomers (0, 5, and 10  $\mu$ M) for 24 h and 72 h. B. Representative images of tunel (green) and DAPI (blue) in primary pericytes incubated with A $\beta$ o for 24 h and 72 h. Scale bar: 50  $\mu$ m. All the data were presented as mean  $\pm$  SEM. \*\*\*\*  $p < 0.0001$

**Additional file 4: Supplementary Table 1.** List of primers used in RNA analyses.

### Acknowledgements

We feel grateful to Professor Wei-Jye Lin at the Brain Research Center of Sun Yat-Sen Memorial Hospital for providing 5xFAD mice.

### Authors' contributions

SC and JC: study design, statistical analysis, results interpretation, and manuscript drafting. SC, JX, DG, ZZ, JH and YH designed and performed the in vivo experiments. SX and YZ wrote ethical permits and performed the in vitro experiments. ZN and XM took part in the writing and editing of the manuscript. YT played a pivotal role in shaping the original research design and direction, influencing the overall scientific narrative of the manuscript. All authors read and approved the final manuscript.

### Funding

This study was funded by the National Natural Science Foundation of China (No. 81925031, 81820108026), Guangzhou Science and Technology Program key projects (202007030001) to Yamei Tang, National Natural Science Foundation of China (82304067), Guangdong Basic and Applied Basic Research Foundation (2021A1515111102) to Jinping Cheng, National Science Foundation of Guangdong Province (2022A1515012396) to Lin Cao.

### Availability of data and materials

The datasets used and/or analysed during the current study are available from the corresponding author on reasonable request.

### Declarations

#### Ethics approval and consent to participate

All experimental procedures were approved by the Sun Yat-sen University Animal Program Animal Care and Use Committee under the Guide for the Care and Use of Laboratory Animals published by the National Institutes of Health.

#### Consent for publication

Not applicable.

#### Competing interests

The authors declare no competing interests.

#### Author details

<sup>1</sup>Department of Anesthesiology, Sun Yat-Sen Memorial Hospital, Sun Yat-Sen University, Guangzhou 510120, China. <sup>2</sup>Department of Neurology, Sun Yat-Sen Memorial Hospital, Sun Yat-Sen University, Guangzhou 510120, China. <sup>3</sup>Brain Research Center, Sun Yat-sen Memorial Hospital, Sun Yat-sen University, Guangzhou 510120, China. <sup>4</sup>Nanhai Translational Innovation Center of Precision Immunology, Sun Yat-sen Memorial Hospital, Foshan 528200, China.

Received: 26 August 2023 Accepted: 28 February 2024

Published online: 12 March 2024

## References

- 2023 Alzheimer's disease facts and figures. *Alzheimers Dement*. 2023;19(4):1598–695.
- Scheltens P, De Strooper B, Kivipelto M, Holstege H, Chételat G, Teunissen CE, et al. Alzheimer's disease. *Lancet*. 2021;397(10284):1577–90.
- Ghosh S, Ali R, Verma S. A $\beta$ -oligomers: a potential therapeutic target for Alzheimer's disease. *Int J Biol Macromol*. 2023;239:124231.
- Raina P, Santaguida P, Ismaila A, Patterson C, Cowan D, Levine M, et al. Effectiveness of cholinesterase inhibitors and memantine for treating dementia: evidence review for a clinical practice guideline. *Ann Intern Med*. 2008;148(5):379–97.
- Huang L-K, Chao S-P, Hu C-J. Clinical trials of new drugs for Alzheimer disease. *J Biomed Sci*. 2020;27(1):18.
- Huang L-K, Kuan Y-C, Lin H-W, Hu C-J. Clinical trials of new drugs for Alzheimer disease: a 2020–2023 update. *J Biomed Sci*. 2023;30(1):83.
- Zhang Y, Chen H, Li R, Sterling K, Song W. Amyloid  $\beta$ -based therapy for Alzheimer's disease: challenges, successes and future. *Signal Transduct Target Ther*. 2023;8(1):248.
- Jeremic D, Jiménez-Díaz L, Navarro-López JD. Past, present and future of therapeutic strategies against amyloid- $\beta$  peptides in Alzheimer's disease: a systematic review. *Ageing Res Rev*. 2021;72:101496.
- Sweeney MD, Sagare AP, Zlokovic BV. Blood-brain barrier breakdown in Alzheimer disease and other neurodegenerative disorders. *Nat Rev Neurol*. 2018;14(3):133–50.
- Biessels GJ. Alzheimer's disease, cerebrovascular disease and dementia: lump, split or integrate? *Brain*. 2022;145(8):2632–4.
- Greenberg SM, Bacskai BJ, Hernandez-Guillamon M, Pruzin J, Sperling R, van Veluw SJ. Cerebral amyloid angiopathy and Alzheimer disease - one peptide, two pathways. *Nat Rev Neurol*. 2020;16(1):30–42.
- Sweeney MD, Zhao Z, Montagne A, Nelson AR, Zlokovic BV. Blood-brain barrier: from physiology to disease and back. *Physiol Rev*. 2019;99(1):21–78.
- Cai Z, Qiao P-F, Wan C-Q, Cai M, Zhou N-K, Li Q. Role of blood-brain barrier in Alzheimer's disease. *J Alzheimers Dis*. 2018;63(4):1223–34.
- Love S, Miners JS. Cerebrovascular disease in ageing and Alzheimer's disease. *Acta Neuropathol*. 2016;131(5):645–58.
- Cong X, Kong W. Endothelial tight junctions and their regulatory signaling pathways in vascular homeostasis and disease. *Cell Signal*. 2020;66:109485.
- Langen UH, Ayloo S, Gu C. Development and cell biology of the blood-brain barrier. *Annu Rev Cell Dev Biol*. 2019;35:591–613.
- Armulik A, Abramsson A, Betsholtz C. Endothelial/pericyte interactions. *Circ Res*. 2005;97(6):512–23.
- Cheng J, Korte N, Nortley R, Sethi H, Tang Y, Attwell D. Targeting pericytes for therapeutic approaches to neurological disorders. *Acta Neuropathol*. 2018;136(4):507–23.
- Winkler EA, Sagare AP, Zlokovic BV. The pericyte: a forgotten cell type with important implications for Alzheimer's disease? *Brain Pathol*. 2014;24(4):371–86.
- Zlokovic BV. Neurovascular pathways to neurodegeneration in Alzheimer's disease and other disorders. *Nat Rev Neurosci*. 2011;12(12):723–38.
- Sweeney MD, Ayyadurai S, Zlokovic BV. Pericytes of the neurovascular unit: key functions and signaling pathways. *Nat Neurosci*. 2016;19(6):771–83.
- Rustenhoven J, Jansson D, Smyth LC, Dragunow M. Brain pericytes as mediators of neuroinflammation. *Trends Pharmacol Sci*. 2017;38(3):291–304.
- Medina-Flores F, Hurtado-Alvarado G, Deli MA, Gómez-González B. The active role of pericytes during neuroinflammation in the adult brain. *Cell Mol Neurobiol*. 2023;43(2):525–41.
- Uemura MT, Maki T, Ihara M, Lee VMY, Trojanowski JQ. Brain microvascular pericytes in vascular cognitive impairment and dementia. *Front Aging Neurosci*. 2020;12:80.
- Nortley R, Korte N, Izquierdo P, Hirunpattarasilp C, Mishra A, Jaunmuktane Z, et al. Amyloid  $\beta$  oligomers constrict human capillaries in Alzheimer's disease via signaling to pericytes. *Science*. 2019;365(6450):eaav9518.
- Jan A, Hartley DM, Lashuel HA. Preparation and characterization of toxic A $\beta$  aggregates for structural and functional studies in Alzheimer's disease research. *Nat Protoc*. 2010;5(6):1186–209.
- Zhang Z, Jiang J, He Y, Cai J, Xie J, Wu M, et al. Pregabalin mitigates microglial activation and neuronal injury by inhibiting HMGB1 signaling pathway in radiation-induced brain injury. *J Neuroinflammation*. 2022;19(1):231.
- Cheng J, Jiang J, He B, Lin W-J, Li Y, Duan J, et al. A phase 2 study of thalidomide for the treatment of radiation-induced blood-brain barrier injury. *Sci Transl Med*. 2023;15(684):eabm6543.
- Yang Y, Li H, Xu Y, Xie J, Liu Q, Shi Z, et al. Notch signaling mediates radiation-induced smooth muscle cell hypermuscularization and cerebral vasculopathy. *Stroke*. 2022;53(12):3751–62.
- Zhao Z, Zhang Y, Zhang C, Zhang J, Luo X, Qiu Q, et al. TGF- $\beta$  promotes pericyte-myofibroblast transition in subretinal fibrosis through the Smad2/3 and Akt/mTOR pathways. *Exp Mol Med*. 2022;54(5):673–84.
- Zudaire E, Gambardella L, Kurcz C, Vermeren S. A computational tool for quantitative analysis of vascular networks. *PLoS ONE*. 2011;6(11):e27385.
- Drummond E, Wisniewski T. Alzheimer's disease: experimental models and reality. *Acta Neuropathol*. 2017;133(2):155–75.
- Armulik A, Genové G, Mäe M, Nisancioglu MH, Wallgard E, Niaudet C, et al. Pericytes regulate the blood-brain barrier. *Nature*. 2010;468(7323):557–61.
- Daneman R, Zhou L, Kebede AA, Barres BA. Pericytes are required for blood-brain barrier integrity during embryogenesis. *Nature*. 2010;468(7323):562–6.
- Winkler EA, Bell RD, Zlokovic BV. Pericyte-specific expression of PDGF beta receptor in mouse models with normal and deficient PDGF beta receptor signaling. *Mol Neurodegener*. 2010;5:32.
- Hayden EY, Teplow DB. Amyloid  $\beta$ -protein oligomers and Alzheimer's disease. *Alzheimers Res Ther*. 2013;5(6):60.
- Wang Z-X, Tan L, Liu J, Yu J-T. The essential role of soluble A $\beta$  oligomers in Alzheimer's disease. *Mol Neurobiol*. 2016;53(3):1905–24.
- Cline EN, Bicca MA, Viola KL, Klein WL. The Amyloid- $\beta$  oligomer hypothesis: beginning of the third decade. *J Alzheimers Dis*. 2018;64(s1):S567–610.
- Schultz N, Nielsen HM, Minthon L, Wennström M. Involvement of matrix metalloproteinase-9 in amyloid- $\beta$  1–42-induced shedding of the pericyte proteoglycan NG2. *J Neuropathol Exp Neurol*. 2014;73(7):684–92.
- Wan W, Cao L, Liu L, Zhang C, Kalionis B, Tai X, et al. A $\beta$ (1–42) oligomer-induced leakage in an in vitro blood-brain barrier model is associated with up-regulation of RAGE and metalloproteinases, and down-regulation of tight junction scaffold proteins. *J Neurochem*. 2015;134(2):382–93.
- Busche MA, Hyman BT. Synergy between amyloid- $\beta$  and tau in Alzheimer's disease. *Nat Neurosci*. 2020;23(10):1183–93.
- Michalíková A, Majerová P, Kováč A. Tau protein and its role in blood-brain barrier dysfunction. *Front Mol Neurosci*. 2020;13:570045.
- Xia M, Jiao L, Wang X-H, Tong M, Yao M-D, Li X-M, et al. Single-cell RNA sequencing reveals a unique pericyte type associated with capillary dysfunction. *Theranostics*. 2023;13(8):2515–30.
- Guo JL, Lee VMY. Cell-to-cell transmission of pathogenic proteins in neurodegenerative diseases. *Nat Med*. 2014;20(2):130–8.
- Sengupta U, Nilson AN, Kaye R. The role of Amyloid- $\beta$  oligomers in toxicity, propagation, and immunotherapy. *EBioMedicine*. 2016;6:42–9.
- Calsolaro V, Edison P. Neuroinflammation in Alzheimer's disease: Current evidence and future directions. *Alzheimers Dement*. 2016;12(6):719–32.
- Rensink AAM, Otte-Höller I, ten Donkelaar HJ, De Waal RMW, Kremer B, Verbeek MM. Differential gene expression in human brain pericytes induced by amyloid-beta protein. *Neuropathol Appl Neurobiol*. 2004;30(3):279–91.
- Chan Y, Chen W, Wan W, Chen Y, Li Y, Zhang C. A $\beta$ 1–42 oligomer induces alteration of tight junction scaffold proteins via RAGE-mediated autophagy in bEnd.3 cells. *Exp Cell Res*. 2018;369(2):266–74.
- Glenner GG, Wong CW. Alzheimer's disease: initial report of the purification and characterization of a novel cerebrovascular amyloid protein. 1984. *Biochem Biophys Res Commun*. 2012;425(3):534–9.
- Giacobini E, Gold G. Alzheimer disease therapy—moving from amyloid- $\beta$  to tau. *Nat Rev Neurol*. 2013;9(12):677–86.
- Panza F, Lozupone M, Logroscino G, Imbimbo BP. A critical appraisal of amyloid- $\beta$ -targeting therapies for Alzheimer disease. *Nat Rev Neurol*. 2019;15(2):73–88.
- Kent SA, Spire-Jones TL, Durrant CS. The physiological roles of tau and A $\beta$ : implications for Alzheimer's disease pathology and therapeutics. *Acta Neuropathol*. 2020;140(4):417–47.
- Congdon EE, Sigurdsson EM. Tau-targeting therapies for Alzheimer disease. *Nat Rev Neurol*. 2018;14(7):399–415.

54. Sims JR, Zimmer JA, Evans CD, Lu M, Ardayfio P, Sparks J, et al. Donanemab in early symptomatic Alzheimer disease: the TRAILBLAZER-ALZ 2 randomized clinical trial. *JAMA*. 2023;330(6):512–27.
55. Rafii MS, Sol O, Mobley WC, Delpretti S, Skotko BG, Burke AD, et al. Safety, tolerability, and immunogenicity of the ACI-24 vaccine in adults with down syndrome: a phase 1b randomized clinical trial. *JAMA Neurol*. 2022;79(6):565–74.
56. Iadecola C. The overlap between neurodegenerative and vascular factors in the pathogenesis of dementia. *Acta Neuropathol*. 2010;120(3):287–96.
57. Bell RD, Zlokovic BV. Neurovascular mechanisms and blood-brain barrier disorder in Alzheimer's disease. *Acta Neuropathol*. 2009;118(1):103–13.
58. Kokmen E, Whisnant JP, O'Fallon WM, Chu CP, Beard CM. Dementia after ischemic stroke: a population-based study in Rochester, Minnesota (1960–1984). *Neurology*. 1996;46(1):154–9.
59. Nation DA, Sweeney MD, Montagne A, Sagare AP, D'Orazio LM, Pachicano M, et al. Blood-brain barrier breakdown is an early biomarker of human cognitive dysfunction. *Nat Med*. 2019;25(2):270–6.
60. Zhao M, Jiang X-F, Zhang H-Q, Sun J-H, Pei H, Ma L-N, et al. Interactions between glial cells and the blood-brain barrier and their role in Alzheimer's disease. *Ageing Res Rev*. 2021;72:101483.
61. Huang Z, Wong L-W, Su Y, Huang X, Wang N, Chen H, et al. Blood-brain barrier integrity in the pathogenesis of Alzheimer's disease. *Front Neuroendocrinol*. 2020;59:100857.
62. Duncombe J, Kitamura A, Hase Y, Ihara M, Kalaria RN, Horsburgh K. Chronic cerebral hypoperfusion: a key mechanism leading to vascular cognitive impairment and dementia. Closing the translational gap between rodent models and human vascular cognitive impairment and dementia. *Clin Sci (Lond)*. 2017;131(19):2451–68.
63. Tachibana M, Yamazaki Y, Liu C-C, Bu G, Kanekiyo T. Pericyte implantation in the brain enhances cerebral blood flow and reduces amyloid- $\beta$  pathology in amyloid model mice. *Exp Neurol*. 2018;300:13–21.
64. Ma Q, Zhao Z, Sagare AP, Wu Y, Wang M, Owens NC, et al. Blood-brain barrier-associated pericytes internalize and clear aggregated amyloid- $\beta$ 42 by LRP1-dependent apolipoprotein E isoform-specific mechanism. *Mol Neurodegener*. 2018;13(1):57.
65. Alcendor DJ. Interactions between Amyloid-**B** proteins and human brain pericytes: implications for the pathobiology of Alzheimer's disease. *J Clin Med*. 2020;9(5):1490.
66. Dehouck MP, Vigne P, Torpier G, Breittmayer JP, Cecchelli R, Frelin C. Endothelin-1 as a mediator of endothelial cell-pericyte interactions in bovine brain capillaries. *J Cereb Blood Flow Metab*. 1997;17(4):464–9.
67. Schultz N, Brännström K, Byman E, Moussaud S, Nielsen HM, Olofsson A, et al. Amyloid-beta 1–40 is associated with alterations in NG2+ pericyte population ex vivo and in vitro. *Aging Cell*. 2018;17(3):e12728.
68. Duan L, Zhang X-D, Miao W-Y, Sun Y-J, Xiong G, Wu Q, et al. PDGFR $\beta$  cells rapidly relay inflammatory signal from the circulatory system to neurons via chemokine CCL2. *Neuron*. 2018;100(1):183–200.
69. Niu F, Liao K, Hu G, Sil S, Callen S, Guo M-L, et al. Cocaine-induced release of CXCL10 from pericytes regulates monocyte transmigration into the CNS. *J Cell Biol*. 2019;218(2):700–21.

## Publisher's Note

Springer Nature remains neutral with regard to jurisdictional claims in published maps and institutional affiliations.